Supporting Information

Facile green synthesis of multifunctional nitrogen-doped carbon dots via sequential non-enzymatic browning reactions for Fe^{3+} sensing and anti-counterfeiting ink

Jiamin Li, [a] Yulu Liu, [a] Yuanyuan Lei, [a] Zehong Ji, [a] Yingzhi Shen, [a] Yuchi Chen, [a] Dongqing Cheng, [a] Wenxiao Jiang, [b] Xing Chen [c] and Guangming Li *[a]

[a.] School of Medical Technology and Information Engineering, Zhejiang Chinese Medical University, Hangzhou, Zhejiang 310053, P. R. China. E-mail: guangmingli2020@163.com

[b.] Department of Nutrition and Food Hygiene, School of Public Health, Shenzhen University Medical School, Shenzhen University, Shenzhen 518055, P. R. China.

[c.] State Key Laboratory of Food Science and Resources, College of Food Science & Technology, Nanchang University, Nanchang, Jiangxi 330047, P. R. China.

* Contact information:
Guangming Li (GML), Tel: +86 15948350475; Fax: N/A; Address: School of Medical Technology and Information Engineering, Zhejiang Chinese Medical University, Hangzhou, Zhejiang 310053, China
E-mail: guangmingli2020@163.com

Supporting Figures

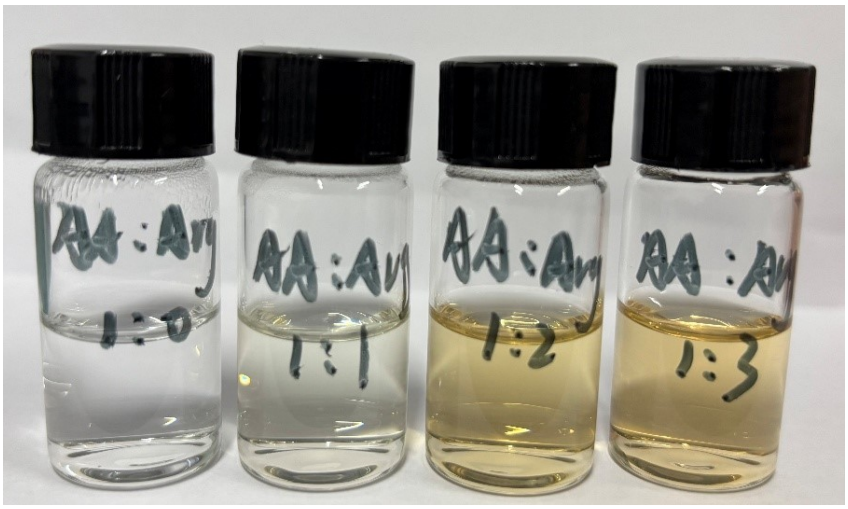

Fig. S1. Photographs of the reaction solutions with different ascorbic acid-to-arginine molar ratios (1:0, 1:1, 1:2, and 1:3) after heating at 60 °C for 5 h. The corresponding pH values were 3–4, 5–6, 9, and 11, respectively. Pronounced browning was observed only at ratios of 1:2 and 1:3 under alkaline conditions (pH 9 and 11).

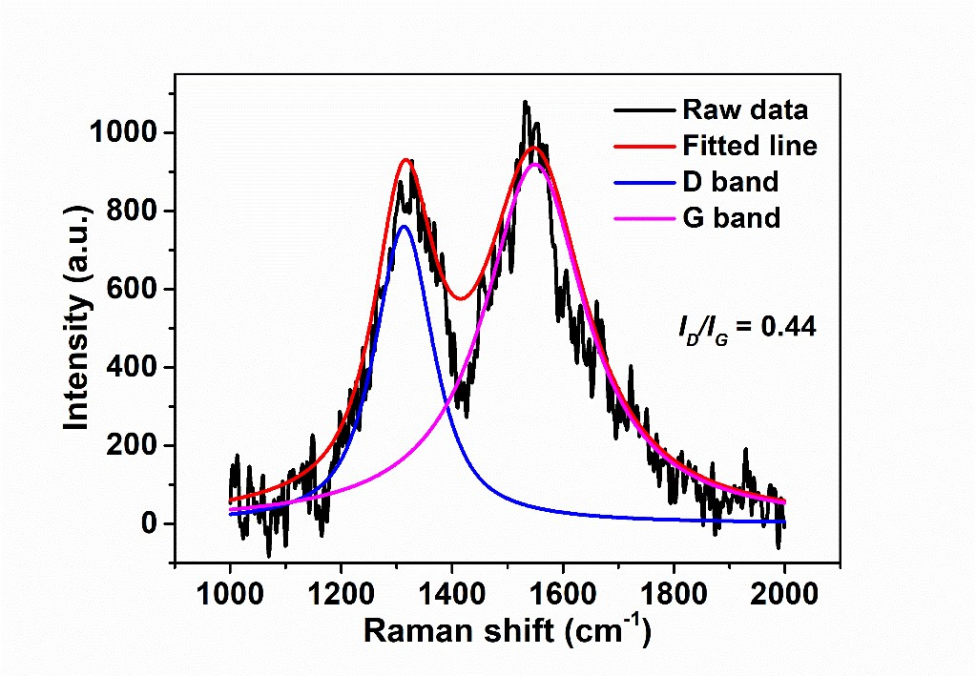

Fig. S2. Raman spectrum of N-CDs. The result shows the D band at 1313.6 cm^{-1} and the G band at 1549.4 cm^{-1}. The I_D/I_G area ratio was calculated to be 0.44, indicating the existence of sp²-hybridized carbon clusters in the N-CDs.

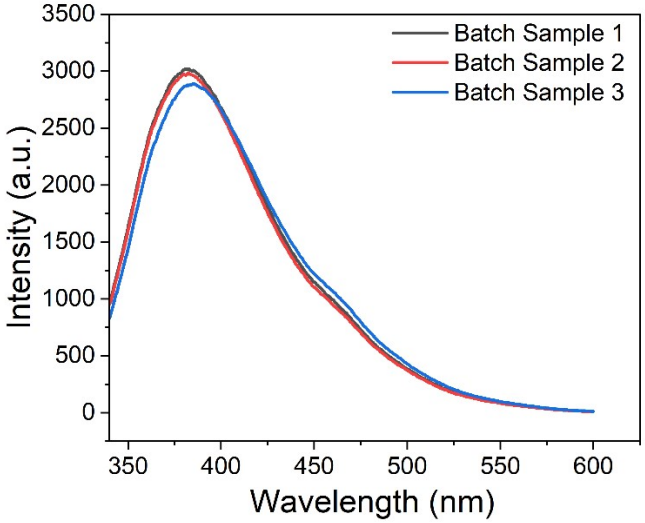

Fig. S3. Fluorescence emission spectra of three independent batches of N-CDs under 320 nm excitation, demonstrating good batch-to-batch reproducibility.

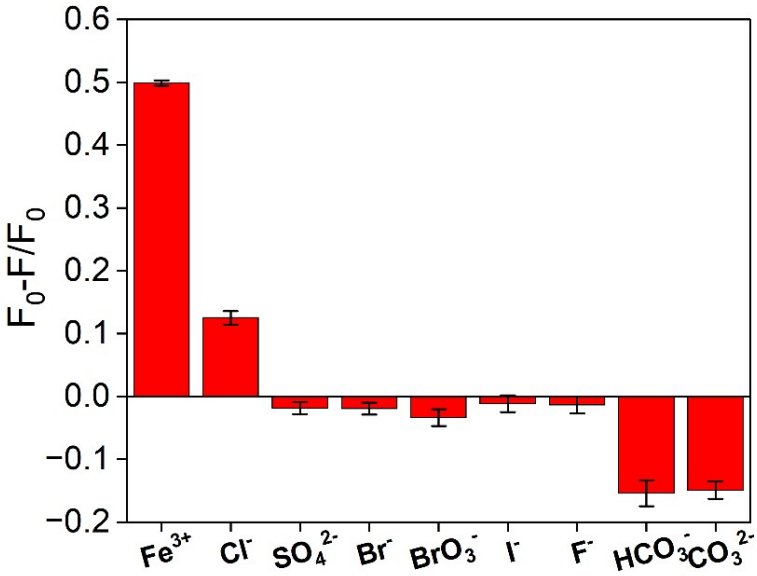

Fig. S4. Fluorescence quenching efficiency of various anions (200 μM). Unlike Fe^{3+}, no significant quenching was observed for the tested anions.

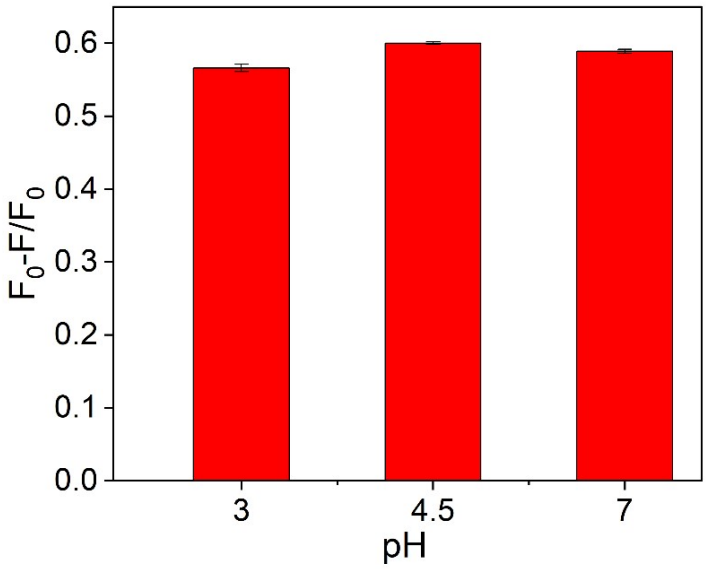

Fig. S5. Effect of initial pH on the Fe^{3+}-induced fluorescence quenching of N-CDs. The quenching efficiency was measured at initial pH 3, 4.5, and 7 after the addition of the same concentration of Fe^{3+}. The quenching efficiency remained almost unchanged across different pH conditions.

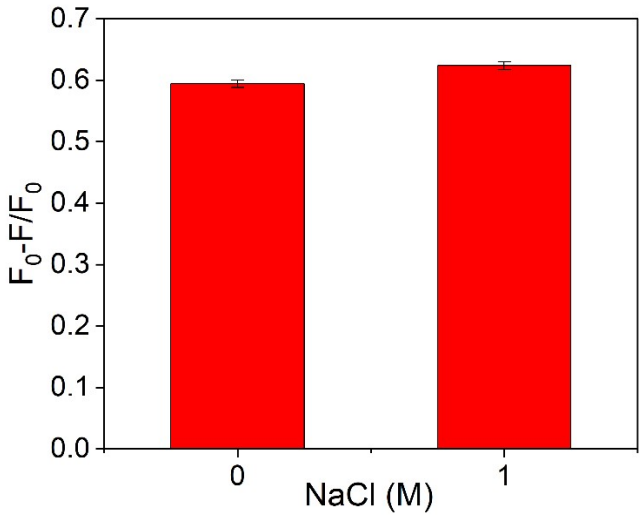

Fig. S6. Effect of ionic strength on the Fe^{3+}-induced fluorescence quenching of N-CDs. The quenching efficiency was evaluated under both original and high-ionic-strength (1 M NaCl) conditions. The quenching efficiency remained almost unchanged under different ionic strength conditions.

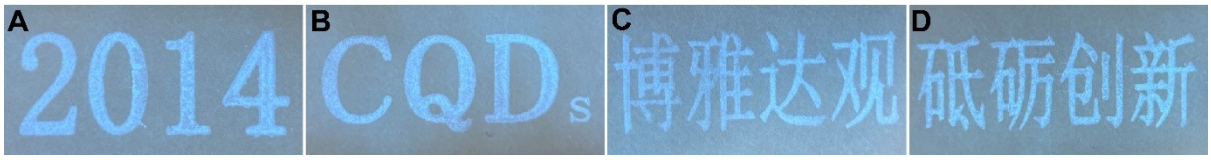

Fig. S7. Fluorescence photographs of the patterns printed with N-CDs-based ink after being stored under ambient conditions for more than six months. The patterns remained bright and sharp with well-defined edges, and no observable fading, bleeding, or loss of fine details was detected, demonstrating the excellent long-term stability of the N-CDs-based ink for anti-counterfeiting applications.

Table S1. Raman spectral parameters of N-CDs: peak, center, areas, intensities, and full width at half maximum (FWHM) of the D and G bands. The I_D/I_G area ratio was calculated to be 0.44.

Peak	Type	Center (cm^{-1})	Area	Intensity	FWHM (cm^{-1})
D band	Gauss+Lor Area	1313.6	142867.6	760.4	127.7
G band	Gauss+Lor Area	1549.4	322912.1	919.1	223.7

Table S2. Elemental composition of N-CDs.

Element	C	N	H	O
Mass (%)	42.39	24.33	6.98	26.30

Table S3: Quenching efficiency comparison of various batches upon addition of Fe^{3+} at 200 μM.

Batch	Fe^{3+} (μM)	F_0-F/F_0	SD
1	200	0.50	
2	200	0.59	0.05
3	200	0.60	

Table S4 Comparison of analytical performance for Fe^{3+} ion detection between our N-CDs and representative non-CDs-based sensors.

Sensors	LOD (μM)	Linear Range (μM)	Analysis time	References
Eu-MOF	2.65	NA	NA	1
MWCNT-modified GCE	6.0	10–100 μM	NA	2
SiNPs	0.56	2.0–50	15 min	3
Polyherbal AgNPs (PH-AgNPs)	7.9	9–54	1 h	4
Tb-MOF (microporous)	4.84	NA	>30 min	5
tKeima fluorescent protein	428.6	Up to ~1500	5 min	6
N-CDs	**2.2**	**10–200**	**<30 s**	**This work**

References

1. Jiao, S., Y. Zhai, H. Zhang, & P. Li. *Polyhedron*, 2025, **281**, 117751.

2. Venegas, C. J., Tamayo, F., Cabrera-Reina, A., Sierra-Rosales, P., & Miralles-Cuevas, S. *Chem. Eng. J. Adv.*, 2026, **26,** 101067.

3. Ye, H. L., Shang, Y., Wang, H. Y., Ma, Y. L., He, X. W., Li, W. Y., Li, Y. H., & Zhang, Y. K. *Talanta*, 2021, **230**, 122294.

4. Vyavahare, A., Shah, P. D., Mishra, V., Patel, A. S., Raina, V., & Jana, S. S. *RSC Adv.*, 2026, **16**, 3976-3994.

5. Zhang, X. F., Feng, L. H., Ma, S. Y., Xia, T. F., Jiao, F. F., Kong, Z., & Duan, X. *J. Solid State Chem.*, 2022, **312**, 123232.

6. Seo, Y. G., Han, D. G., & Kim, I. J. *Biosensors*, 2026, **16**, 178.